Glacier surface mass balance modeling in the inner tropics using a positive degree-day approach

L. Maisincho[1,2], V. Favier[3], P. Wagnon[2,4], V. Jomelli[5], R. Basantes Serrano[2,3], B. Francou[2], M. Villacis[6], A. Rabatel[3], M. Ménégoz[7], L. Mourre[2], B. Cáceres[1]

[1] INAMHI, Instituto Nacional de Meteorología e Hidrología, Iñaquito N36-14 y Corea, Quito, Ecuador.

[2] IRD/Univ. Grenoble Alpes/CNRS/INPG, Laboratoire d'étude des Transferts en Hydrologie et Environnement (LTHE), UMR5564, Grenoble 38041, France.

[3] Univ. Grenoble Alpes, CNRS LGGE (UMR5183), F-38000 Grenoble, France.

[4] ICIMOD, GPO Box 3226, Kathmandu, Nepal

[5] LGP, Université Paris 1 Panthéon-Sorbonne-CNRS, 92195 Meudon, France.

[6] EPN, Escuela Politécnica Nacional, Ladrón de Guevara E11-253, Quito, Ecuador.

[7] Institut Català de Ciènces del Clima (IC3), Doctor Trueta, 203 3a planta 08005 Barcelona (Spain)

Supplementary Materials

1 Surface energy balance model

Daily ablation from the basic model based on the PDD approach was calibrated with surface energy balance values computed for a horizontal surface using the Favier *et al.*

(2011) approach from March 14, 2002 to August 31, 2003 (Figure S1) and from January 1, 2005 to November 30, 2005. The energy used for melting or stored in the top layers of the glacier was calculated as (fluxes toward the surface are positive) (Favier *et al*., 2011; Azam *et al*., 2014):

$$S\downarrow + S\uparrow + L\downarrow - ((1-\varepsilon)\, L\downarrow + \varepsilon\, \sigma\, T_s^4) + LE + H = Q_{surface} \quad \text{(in W m}^{-2}\text{)} \qquad (3)$$

where $S\downarrow$ is incoming shortwave radiation, $S\uparrow$ is reflected short-wave radiation; $L\downarrow$ is incoming long-wave radiation and the term in brackets is outgoing longwave radiation $L\uparrow$; H and LE are respectively, turbulent sensible and latent heat fluxes, which were computed using the bulk method including stability corrections based on the bulk Richardson number. We used the surface roughness length given by Favier *et al*. (2004a) considering the equality of values for momentum, moisture, and temperature. Air temperature and humidity were measured using an artificially ventilated HMP45 Vaisala sensor and wind speed was measured using a Young 05103 anemometer (Table 1). The incoming radiative fluxes and the albedo were measured locally at 4,900 m a.s.l. on Antizana Glacier 15 with a CNR1 Kipp & Zonen net radiometer. $L\uparrow$ was deduced from the modeled surface temperature T_s and Stefan-Boltzmann's equation, where $\varepsilon = 0.99$ is surface emissivity, and $\sigma = 5.67\ 10^{-8}$ W m^{-2} K^{-4} is the Stefan-Boltzmann constant. The heat flux supplied by precipitation was not taken into account because during precipitation the temperature is always close to 0 °C.

$Q_{surface}$ is the energy available at the surface. Part of the net shortwave radiation (S) is actually not available for warming/cooling processes at the surface or for melting, because

the shortwave flux partly penetrates the ice. Hence, $Q_{surface}$ is separated into two terms:

$$Q_{surface} = G_0 + (1 - a)\, S \qquad \text{(in W m}^{-2}\text{)} \qquad (4)$$

where G_0 is energy excess or deficit at the surface. In this equation, a is the fractional amount of shortwave radiation that is absorbed in the top layer of the model (at the surface). We assumed a = 0.8 for ice and a = 0.9 for snow (e.g., Bintanja *et al*. 1997). When the surface temperature is 0 °C, the positive G_0 values represent the energy available for melt. Otherwise, this amount is used to cool/warm the frozen surface and underlying snow/ice. For this task, heat conduction within the snow or ice was computed by solving the thermal diffusion equation according to an explicit scheme to a depth of 2 m, with a 5 cm grid resolution and a 20 s time step.

Calculations were validated using the melting amounts measured by the melting boxes (Figure S2c). Our results were in better agreement with measured melting amounts than results from Favier et al. (2004), with a correlation coefficient of r = 0.91 (instead of 0.86). The regression line was also closer to the 1:1 line (slope of 1.01 instead of 0.89). The model was also validated using mass balance measurements performed on ablation stakes. Because the ablation zone presents a significant slope (28°) and aspect (NW) for this elevation range, the surface energy balance model was run with these settings from March 14, 2002 to August 31, 2003. The computed monthly mass balance values were highly consistent with the mass balance values measured on the stakes (r = 0.90, n = 18, p = 0.001, E = 0.79, Figure S2).

2 Correlation analysis

The daily and monthly mean values of temperature and of energy fluxes of AWS_{G1}, from March 14, 2002 to August 31, 2003 were used for the correlation analysis presented in Supplementary Section 1.1.1 and 1.1.2.

2.1 Correlation at a monthly time scale

We first calculated the correlations between incoming energy fluxes, precipitation, and temperature at a monthly time scale for the period March 2002 to August 2003 for which all surface energy fluxes were available (Table S1). Correlation coefficients were also computed with wind speed because this variable has a marked impact on ablation processes on Antizana Glacier 15. The cumulative half-hourly positive temperature values over one month are noted $T+$.

At the AWS_{G1} monthly mean temperature was usually poorly correlated with the incoming energy fluxes ($S\downarrow$, $L\downarrow$, *LE, H)*. However, correlations with $S\uparrow$ and $L\uparrow$ were more significant that for incoming fluxes, which reflected the impact of low temperature on high albedo values and on reduced melting. Interestingly, wind velocity was also correlated with local incoming fluxes (Table S1), but, surprisingly, wind speed was not correlated with albedo, net radiation, or melting (Table S1). In fact, variations in incoming fluxes were not able to explain the variations in melting (Table S1). Melting was almost totally controlled by variations in albedo (Table S1, see also correlations between melting and S and the net radiation (R)). Significant correlations were found between precipitation and S and albedo, suggesting that precipitation is a key variable when modeling mass balances in Ecuador.

Finally, a significant correlation was found between $T+$ and melting. This link was

already suggested by results obtained by Francou *et al*. (2004) (between January 1995 and December 2002), who proposed that monthly temperature and solid precipitation had a first order control on albedo variations on Antizana Glacier 15 specific mass balance.

2.2 Correlation at a daily time scale

Over the 2002-2003 period, net shortwave radiation was by far the most important variable involved in melting processes (r = 0.88, n = 530, p = 0.001) (Table S2, see also Favier *et al*. (2004a&b) for details). Thus, melting may only be quite accurately modeled with this variable. Reproducing albedo variations is thus crucial over Ecuadorian glaciers. Here we observed that daily albedo values were only significantly correlated with daily temperature (even if the correlation was rather poor i.e. r = -0.53 with T or with cumulative half-hourly positive temperature over one day, T+, at p = 0.001), reflecting the important impact of the 0 °C level on the precipitation phase and explaining why melting is also significantly correlated with temperature (r = 0.62, with T and T+). Conversely, no correlations were found between melting and wind speed or precipitation (Table S2). Writing a model based on daily temperature variations thus appears to some extent justified here.

To go a step further in this analysis, we investigated whether the correlations between temperature and melting or incoming heat fluxes remained constant over the year, or depended on meteorological conditions closely related to wind speed.

We observed that the correlations between temperature, $S\downarrow$, $L\downarrow$, LE or H and melting were effectively influenced by strong winds. Indeed, when we divided the study period according to wind speed (i.e. windy Period 1 versus calm Period 2), $S\downarrow$ and $L\downarrow$ (which were together significantly correlated (r = -0.73, n = 530) due to the impact of clouds) were

significantly correlated with T and with melting in Period 2 (Table S2), and during days with low-speed winds that sometimes occurred during Period 1 (i.e., when the wind speed, $\bar{u}$, was less than 4 m s^{-1}). Indeed, on calm days, the turbulent heat fluxes and the resulting air mixing were not strong enough to affect the relationship between enhanced $S\downarrow$, melting, and surface warming. However, this relationship collapsed with strong winds because turbulent heat fluxes played an increasing role in the surface heat budget that controlled the melting processes.

These observations were confirmed by a detailed analysis of the relationships between cumulative half-hourly positive temperatures and the various energy balance fluxes on selected days when direct field melting measurements were available (Figure S3). Indeed, the cumulative hourly positive temperature values were significantly correlated (at p = 0.001) only with incident shortwave radiation and with the net shortwave radiation during calm periods. When turbulent fluxes were strong due to strong winds, these correlations disappeared.

In conclusion, moderate but significant (at p=0.001) correlations between air temperature, S and albedo, do exist and correlations between temperature and $S\downarrow$ are significant but only during low-speed wind periods.

2.3 Correlation between sublimation and wind speed

Turbulent heat fluxes are difficult to estimate with temperature, but LE was significantly correlated with the daily wind speed (r = -0.79, n = 530, p = 0.001, see Table S2). This rather high correlation was already used by Favier *et al*. (2008) and Soruco *et al*. (2009) to assess sublimation on glaciers. The regression line between the daily wind speed and turbulent latent heat flux enables daily sublimation to be written as follows:

$$Sublimation = LE*24*3600 / L_s = -5.73\ u \quad (\text{in kg m}^{-2} \text{ or mm w.e.}) \qquad (7)$$

where u is daily mean wind speed (in m s^{-1})and L_s is latent heat constant for sublimation (2.834 10^6 J kg^{-1}). Application of this equation gives a cumulative sublimation of 446 mm w.e. in 2002-2003 (530 days), compared to 420 mm w.e. given by computing the full turbulent heat fluxes. In 2002-2003, this simple model for sublimation presented an efficiency of E = 0.58 with sublimation values given by the bulk method. Equation (7) was validated using data from 2005. The correlation between estimated sublimation and the results of the computation of full turbulent heat fluxes was still significant (r = 0.78, n = 334, p = 0.001), and a similar cumulative sublimation amount was observed with the simplified method (250 mm w.e.) and with the bulk method (284 mm w.e.). Finally, the Nash test gave E=0.53, which is still acceptable given the simplicity of our relationship.

Supplementary Tables

Table S1**:** Correlation coefficients (r) computed between monthly temperature, cumulative half-hourly positive temperature (*T*+), precipitation, and the different incoming energy fluxes measured at AWS_{G1} between April 2002 and August 2003. Correlation coefficients that are significant at p=0.001 level are in bold.

r	*Melt* *(mm w.e.)*	$S_{\downarrow}$ *(J m^{-2})*	$S_{\uparrow}$ *(J m^{-2})*	*S* *(J m^{-2})*	α	$L_{\downarrow}$ *(J m^{-2})*	$L_{\uparrow}$ *(J m^{-2})*	*L* *(J m^{-2})*	*R* *(J m^{-2})*	*H* *(J m^{-2})*	*LE* *(J m^{-2})*	*LE+H* *(J m^{-2})*
T, AWS_{G1}, °C	0,69	-0,55	**0,81**	0,22	-0,62	0,51	**-0,76**	0,46	0,54	-0,62	0,68	0,42
T+, AWS_{G1}, °C	**0,73**	-0,43	**0,76**	0,32	-0,67	0,39	-0,67	0,33	0,59	-0,49	0,56	0,40
Precipitation, *HOBO*, mm	-0,60	-0,21	-0,42	**-0,73**	**0,74**	0,32	0,02	0,36	-0,68	-0,10	0,26	0,49
u, AWS_{G1}, m s^{-1}	-0,17	**0,93**	**-0,76**	0,30	0,25	**-0,84**	**0,80**	**-0,82**	-0,12	**0,95**	**-0,87**	-0,16
ΔQ, mm eq.e,		0,02	**0,70**	**0,80**	**-0,91**	0,05	-0,50	-0,02	**0,97**	-0,24	0,17	-0,11

Table S2**:** Correlation coefficients (*r*) computed between daily temperature, cumulative half-hourly positive temperature (*T*+), melting (ΔQ), wind speed (*u*) and the different energy fluxes measured at AWS_{G1} from March 14, 2002 to August 31, 2003 period (n = 530 days). The period with high speed winds (Period 1) and low speed winds (Period 2) (P1 and P2 in the Table) represent 240 and 290 days, respectively. Additional separation is done for Period 1 to keep observations with low speed winds (see data in brackets). Selected days were when the mean 7-day running mean of wind speed was less than 4 m s^{-1} (51 days). Correlations in bold are significant at p = 0.001.

r	*Significant at 0.001 if |r| higher than values in this column*	*Melt (mm w.e.)*[2]	$S_{\downarrow}$ *(J m^{-2})*	$S_{\uparrow}$ *(J m^{-2})*	*S (J m^{-2})*	*α*	$L_{\downarrow}$ *(J m^{-2})*	$L_{\uparrow}$ *(J m^{-2})*	*L (J m^{-2})*	*R (J m^{-2})*	*H (J m^{-2})*	*LE (J m^{-2})*	*LE+H (J m^{-2})*[2]
T, °C, P1+P2	0.15	**0.62**	0.13	**0.37**	**0.45**	**-0.53**	**-0.16**	**-0.23**	**-0.21**	**0.46**	0.09	0.14	**0.45**
P1(P1 & $\bar{u}$ < 4 m s^{-1})	0.22(0.45)	**0.60(0.48)**	0.15(**0.43**)	**0.39**(0.09)	**0.47(0.48)**	**-0.53(-0.44)**	**-0.28(-0.54)**	-0.13(0.22)	**-0.32(-0.56)**	**0.43(0.36)**	0.07(**0.52**)	0.05(-0.25)	**0.23**(0.28)
P2	0.20	**0.60**	**0.45**	0.11	**0.56**	**-0.50**	**-0.47**	-0.02	**-0.51**	**0.46**	**0.53**	-0.20	**0.60**
T+, °C, P1+P2	0.15	**0.62**	0.21	**0.29**	**0.49**	**-0.53**	**-0.23**	-0.10	**-0.27**	**0.47**	0.08	0.13	**0.43**
P1(P1 & $\bar{u}$ < 4 m s^{-1})	0.22(0.45)	**0.58(0.54)**	0.16(**0.48**)	**0.34**(0.10)	**0.44(0.53)**	**-0.49(-0.47)**	**-0.26(-0.56)**	-0.04(0.25)	**-0.29(-0.58)**	**0.41(0.42)**	0.04(0.44)	0.08(-0.21)	**0.25**(0.24)
P2	0.20	**0.61**	**0.51**	0.07	**0.60**	**-0.51**	**-0.54**	0.12	**-0.57**	**0.48**	0.44	-0.14	**0.54**
Precipitation, mm, P1+P2	0.15	**-0.28**	-0.20	-0.13	**-0.34**	**0.37**	**0.32**	**-0.16**	**0.33**	**-0.25**	**-0.19**	0.13	-0.09
P1(P1 & $\bar{u}$ < 4 m s^{-1})	0.22(0.45)	**-0.30**(-0.39)	-0.23(-0.06)	-0.15(-0.44)	**-0.36**(-0.40)	**0.38(0.47)**	**0.40**(0.32)	-0.12(-0.07)	**0.41**(0.35)	**-0.24**(-0.35)	-0.24(-0.07)	0.17(0.15)	-0.07(0.10)
P2	0.20	**-0.30**	-0.19	-0.17	**-0.32**	**0.39**	**0.29**	**-0.22**	**0.28**	**-0.27**	-0.14	0.06	-0.14
u, m s^{-1}, P1+P2	0.15	0.05	**0.66**	**-0.53**	**0.32**	0.03	**-0.53**	**0.27**	**-0.54**	0.09	**0.82**	**-0.79**	-0.04
P1(P1 & $\bar{u}$ < 4 m s^{-1})	0.22(0.45)	-0.17(-0.05)	**0.62**(0.18)	**-0.56**(-0.18)	0.18(0.04)	0.11(0.07)	**-0.50**(-0.11)	0.22(-0.19)	**-0.50**(-0.17)	-0.06(-0.03)	**0.79(0.62)**	**-0.75(-0.62)**	-0.13(-0.01)
P2	0.20	**0.43**	**0.52**	-0.17	**0.45**	**-0.22**	**-0.32**	-0.11	**-0.36**	**0.40**	**0.75**	**-0.75**	**0.21**
ΔQ, mm eq.e,, P1+P2	0.15		**0.44**	**0.46**	**0.88**	**-0.86**	**-0.29**	**-0.19**	**-0.34**	**0.94**	0.15	-0.02	**0.23**
P1(P1 & $\bar{u}$ < 4 m s^{-1})	0.22(0.45)		**0.34(0.62)**	**0.62(0.49)**	**0.85(0.97)**	**-0.90(-0.92)**	**-0.33(-0.55)**	**-0.22**(-0.11)	**-0.38(-0.64)**	**0.91(0.96)**	0.01(0.14)	-0.02(-0.33)	-0.03(-0.22)
P2	0.20		**0.73**	**0.26**	**0.97**	**-0.83**	**-0.52**	-0.01	**-0.56**	**0.96**	**0.52**	**-0.34**	**0.40**

Supplementary Figures

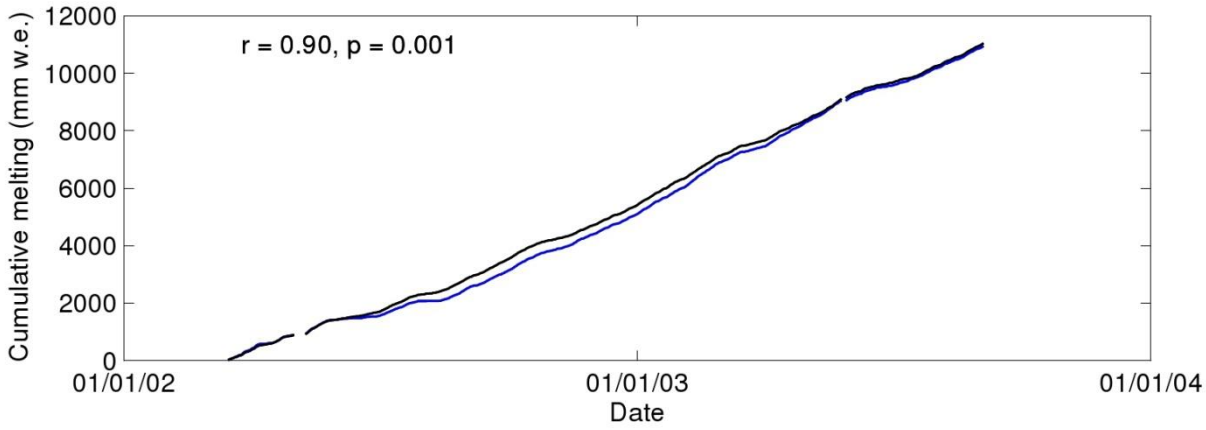

Figure S1: Comparison between cumulative melting rates from Favier et al., (2004) and melting rates computed using Favier et al. (2011) full surface energy balance computation. The correlation coefficient is between daily melting rates of both methods.

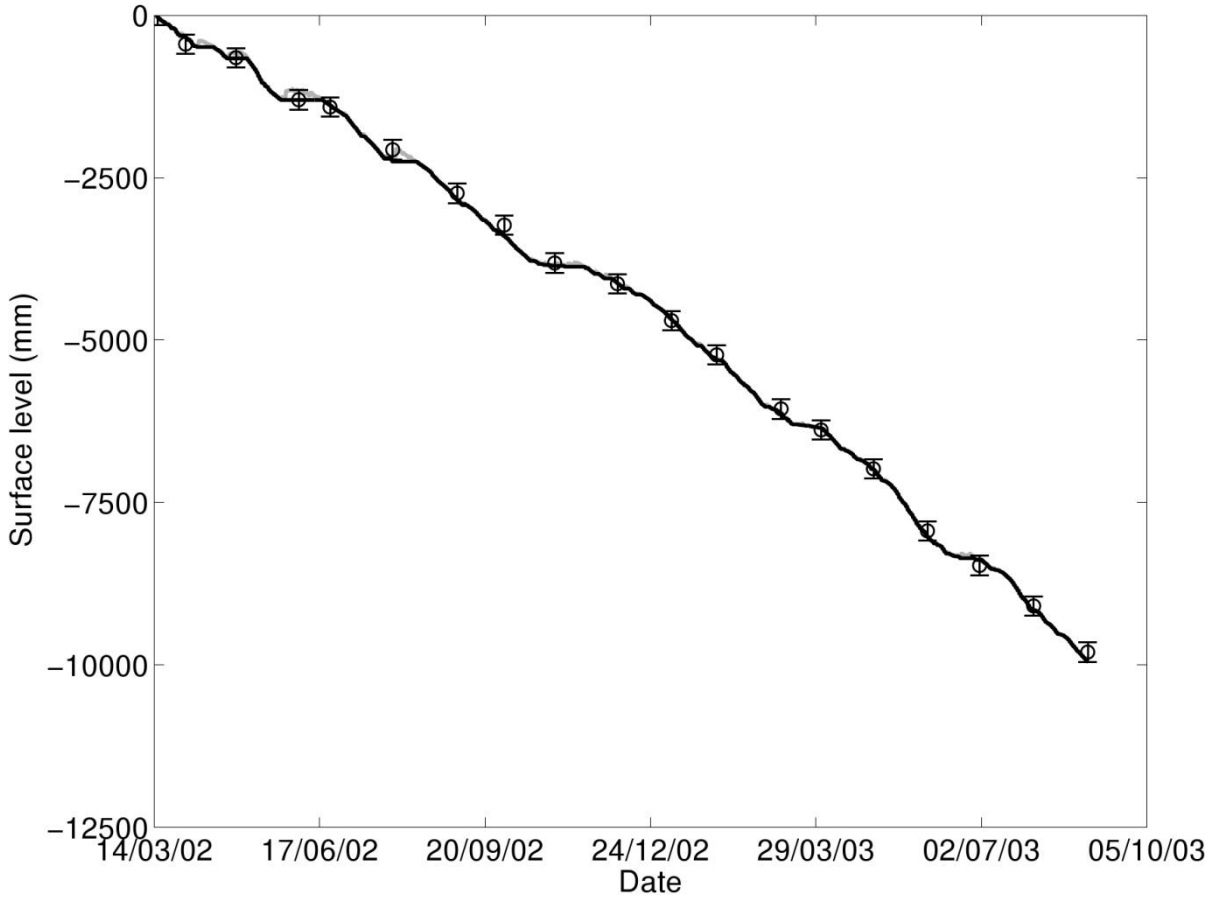

Figure S2: Comparison between measured (circles) and modeled (black lines) surface mass balance and using the full surface energy balance approach in Favier et al. (2011) (values expressed in m of ice). Results are for 4,900 m a.s.l from March 14, 2002 to August 31, 2003. The gray line represents the level of snow assuming a density of 200 kg m^{-3}.

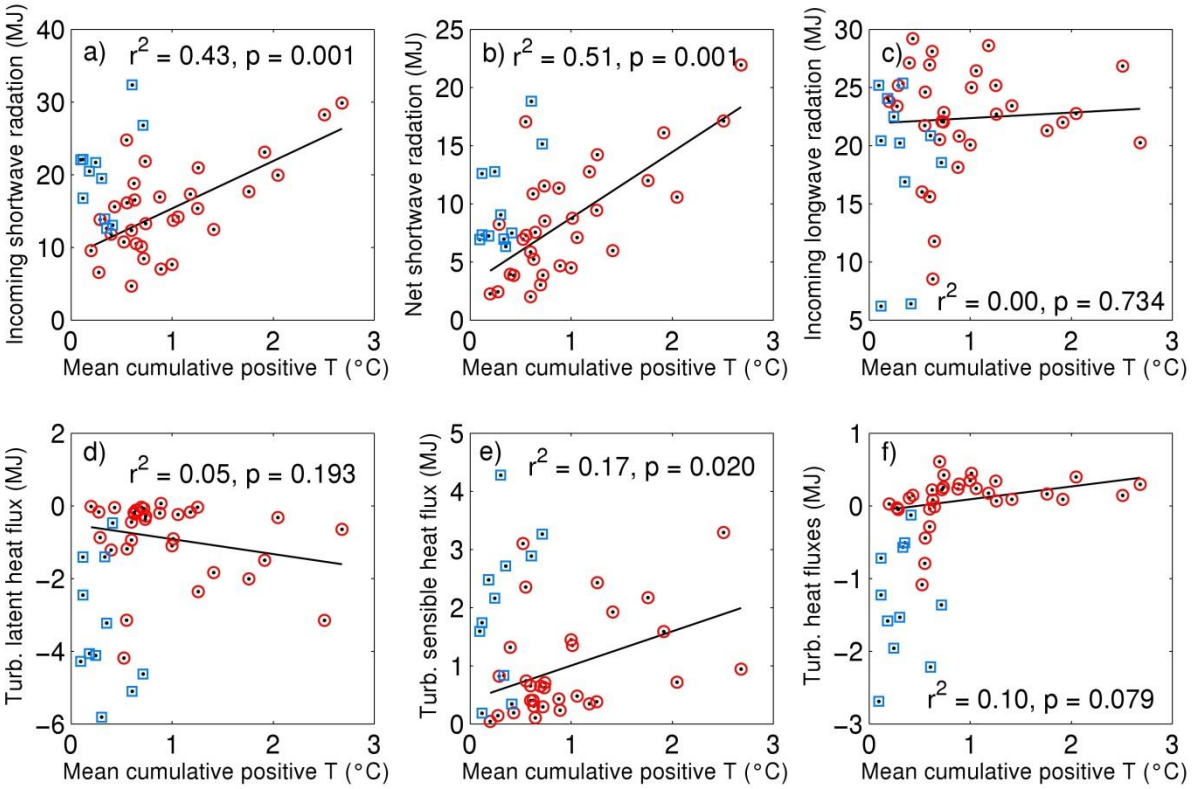

Figure S3: Comparison between the mean cumulative half-hourly positive temperature values in the melting box experiments and a) incoming shortwave radiation, b) net shortwave radiation, c) incoming longwave radiation, d) turbulent latent heat flux, e) turbulent sensible heat flux, and f) turbulent heat fluxes (LE+H). Blue squares refer to Period 1 (windy period) and red circles refer to Period 2. The determination lines and coefficients correspond to data for Period 2 only.